ScienceAsia 28 (2002) : **49-54**

Scaling Laws for the Wavelength and the Appearance Time of Cells Resulting from Double-Diffusive Convection

Karsten Kötter[a] and Mario Markus[a,*]
Max-Planck-Institut für molekulare Physiologie Postfach 500247, D-44202 Dortmund, Germany.
* Corresponding author, E-mail: mario.markus@mpi-dortmund.mpg.de

Received 25 May 2001
Accepted 28 Sep 2001

ABSTRACT We investigate the solutions of partial differential equations describing a two-layered fluid system. The lower layer contains a fastly diffusing, stabilizing substance *T* and a slowly diffusing, destabilizing substance S. The upper layer contains only the solvent. Double-diffusive convection yields cells in agreement with experiments performed with a tenside (*S*) and glycerine (*T*) dissolved in water. Approximation of the PDEs renders scaling laws for the appearance time T_{em} of the cells and their wavelength λ, as functions of the initial concentrations S_0 and T_0, as well as λ as a function of time. These approximations agree well with the solutions of the PDEs.

KEYWORDS: double-diffusive convection, salt fingers, self-organization

INTRODUCTION

Double-diffusive convection results from an instability at an interface between two fluid layers.[1-3] Such layers contain different amounts of a slowly diffusing, gravitationally destabilizing dissolved substance *S* and a fastly diffusing, stabilizing dissolved substance *T*. The instability is counterintuitive at first glance; in fact, if one considers only the total densities and not their composition, the layers would be stable.

A fluctuation at the interface causing a protrusion *P* from layer L_1 to layer L_2, may be depleted of *T* fastly enough by diffusion, so that *S* in *P* can abandon L_1 and *P* grows. As examples for two horizontal layers: i) *S* (heavier than water, but diffusing slowly) and *T* (lighter than water, but diffusing fastly) are layered above water; ii) *S* (lighter than water, but diffusing slowly) and *T* (heavier than water, but diffusing fastly) are layered below water.

In general, the protrusions initially self-organize into a cell structure at the interface.[4] Later on, protrusions grow as fingers from the vertices of the cells. Such a process causes deeply disposed sewage to rise upwards from the bottom of the sea[2, 5], it occurs at melting icebergs (a situation relevant to the projects of obtaining fresh water from icebergs towed to warmer coasts)[6-8], it disturbs the homogeneous crystallisation of alloys[9], and it accounts for the formation of salt fingers at the outflow of the mediterranean over the Atlantic[10, 11] (situation i) in the last paragraph); also, it appears in calculations of the stellar interiors[12] and the earth's magma.[13] Typical quantitative characteristics of a variety of systems are given in.[14]

PARTIAL DIFFERENTIAL EQUATIONS AND THEIR EXPERIMENTAL PARAMETRIZATION

We consider the general PDEs for an incompressible, hydrodynamic system with two dissolved substances *S* and *T*:

$$\partial/\partial t\,\vec{v} + (\vec{v}\vec{\nabla})\vec{v} = \rho/\rho_0\,\vec{g} - 1/\rho_0\,\vec{\nabla}p + \nu\Delta\vec{v} \quad (1)$$

$$\vec{\nabla}(\rho\vec{v}) = 0 \quad (2)$$

$$\partial/\partial t\,S + (\vec{v}\vec{\nabla})S = D_S\Delta S \quad (3)$$

$$\partial/\partial t\,T + (\vec{v}\vec{\nabla})T = D_T\Delta T \quad (4)$$

$$\rho/\rho_0 = 1 + \alpha_T T - \alpha_S S \quad (5)$$

D_T and D_S are the diffusion coefficients, p the pressure, $\vec{v}$ the fluid velocity, ρ its density, ρ_0 the density of the solvent, ν the kinematic viscosity, $\alpha_T = (\rho_T - \rho_0)/\rho_0$, $\alpha_S = (\rho_0 - \rho_S)/\rho_0$. Eq (1) is the Navier-Stokes equation, Eq (2) the equation of continuity, Eqs (3) and (4) describe the diffusion and advection of *S* and *T*, Eq (5) is the equation of state. In 3D, these are 6 scalar equations for the variables $\vec{v}$, *S*, *T* and *p*. At $t = 0$ we set a linear height profile for *S* and *T* ranging from T_0 and S_0 at $z = 0$ to 0 for $z \geq 0.3$ mm; $\vec{v}$ at t = 0 was set to $\vec{0}$. T_0 and S_0 at $t = 0$ were

varied throught this work. In order to initialize the unstable behaviour, we superposed equally distributed noise with a relative amplitude of 1% on the variables S and T at $t = 0$. The equations were integrated using the finite volume method on a colocated grid with an implicit three time level scheme, central difference scheme and the SIMPLE algorithm for pressure correction.[15] We set periodic boundary conditions in x and y direction; at the bottom and the top we imposed no-slip boundary conditions for the velocity and no-flux boundary conditions for the solutes. We set the uniform grid size to $5\text{x}10^{-3}$ mm and the simulated domain to 0.8x 0.8x0.8 mm^3 for initial conditions leading to wavelengths below 0.25 mm; otherwise, we set a grid size of $1\text{x}10^{-2}$ mm and a domain of 1.2x1.2x1.2 mm^3. The time step was set to $\Delta t = 0.05$ s for setups leading to typical pattern formation times below 300 s and $\Delta t = 0.1$ s otherwise.

Experiments and PDE solutions

In order to solve Eqs (1)-(5) numerically we need parameters of a concrete physical system. We consider a system that we have deviced ourselves, having the advantage that it costs only a few dollars and leads to structures within minutes; note that processes of this kind may take hours[16] or days.[4] The cells in our device can be observed with an ordinary light microscope; needle-like fingers growing out from the vertices of these cells are visible to the bare eye. In this system, the solvent is water, T is glycerin and S is an alcohol ethoxylate (nonionic tenside) with 12 carbons in the hydrophobic chain and 16 carbons in the hydrophilic chain.[17] $\alpha_T = 26$ vol%$^{-1}$, $\alpha_S = 5$ vol%$^{-1}$. We set $\nu = 1.1\text{x}10^{-6}$m^2/s; capillary viscosimeter measurements showed that this value does not vary significantly within the ranges of S and T considered here. The diffusion coefficient of glycerine is $D_T = 10^{-10}$m^2/s.

We performed X-ray small angle scattering measurements. These measurements revealed that the tenside forms micelles having the shape of long rods (diameter ≈ 48 Å, length ≈ 4000 Å). The elongation of the micelles increases the diffusion coefficient by a factor of 3.4, as compared to that of a sphere of equal diameter.[18] The elongation of glycerine molecules can be neglected in this respect, so that one can approximate them by a sphere having a diameter of 5 Å. Considering that the diffusion coefficient of a sphere is inversely proportional to its radius (Stokes law), we can estimate here $D_T/D_S \approx 33$ and we thus set $D_S = 3\text{x}10^{-12}$m^2/s.

The integration of Eqs (1)-(5), setting $S_0 = 5$ vol%, $T_0 = 5$ vol% and using the parameters given above yielded Fig 1a. These simulations compare well with experiments (Fig 1b) using the setup described in the figure caption.

Approximations and scaling laws

In this section we will derive simple, approximate exponential expressions (scaling laws) for the time of appearance T_{em} of the cells, as well as for their wavelength λ at $t = T_{em}$, as functions of the initial concentrations T_0 and S_0. In the next section we will compare these scaling laws with the exact results obtained by numerical integration of the PDEs. In previous works, scaling laws for the height of the fingers, as well as for the flux of the substances have been reported.[19, 20]

If a linear analysis is performed around the solution of the equations at time t, perturbations grow ~ $\exp(\Lambda(z, t)\, t)$. (We hold x and y at some fixed, but arbitrary value). In experiments the z-dependence is eliminated by evaluating the total vertically absorbed light intensity. The absorbtion process follows a geometrical progression as light proceeds from one infinitesimal layer to the next. The product (over all infinitesimal layers along the z-direction) of the exponentially growing perturbation is thus $\exp(\Lambda(t))$,
where

$$\Lambda(t) = \int_0^{h(t)} \Lambda(z,t)\,dz. \qquad (6)$$

Here, $h(t)$ is the maximum z at which double-diffusive convection occurs. For our evaluation of the PDE solutions (determination of the cell appearance time and the wavelength) we programmed the elimination of the z-dependence that we just described, so that the PDE evaluation is comparable to experimental observations. $h(t)$ is determined as the maximum value of z at which the condition

$$(\alpha_S \beta_S)/(\alpha_T \beta_T) > D_S / D_T \qquad (7)$$

for double-diffusive convection[21] is fulfilled. $\beta_T = -\partial T/\partial z, \beta_S = -\partial S/\partial z.$

We want to determine the time T_{em} for which an evaluated perturbation has grown by a given factor F. Thus,

$$F = \lim_{\Delta t \to 0} \prod_{i=1}^{N} \exp\,(\Lambda(t)\Delta t) = \lim_{\Delta t \to 0} \exp\left(\sum_{i=1}^{N} \Lambda(t)\Delta t \right)$$

$$= \exp\left[\int_0^{T_{em}} \Lambda(t)dt\right], \quad (8)$$

where $N = T_{em}/\Delta t$. Inserting Eq (6) in Eq (8) leads to

$$F = \exp\left[\int_0^{T_{em}} \int_0^{h(t)} \Lambda(z,t)dz\,dt\right]. \quad (9)$$

Λ has been estimated by Stern[21] as

$$\Lambda = \frac{1}{2}\sqrt{\frac{gD_T}{\nu\alpha_T\beta_T}}\alpha_S\beta_S. \quad (10)$$

Furthermore, Stern[21] estimated the wavelength as

$$\lambda \approx \pi\left(\frac{4\nu D_T}{g\alpha_T}\right)^{\frac{1}{4}}\beta_T^{-\frac{1}{4}}. \quad (11)$$

In the works published so far, one has not considered that Stern's approximations are functions of time owing to the fact that the concentration gradients β_T and β_S change due to diffusion. We will correct this in the present work by considering the evolution of the spatial profile of S and T in z-direction. We thus aim to obtain $\Lambda(z, t)$ from Eq (10) by proper substitutions of β_C ($C : S, T$). For sufficiently large times, and consistently with the times considered in this work, the diffusion equation renders the profile

$$C(z,t) = \frac{HC_0}{2\sqrt{\pi D_C t}}\exp\left[-z^2/(4D_C t)\right], \quad (12)$$

H is the initial height. Eq (12) allows to calculate $\beta_C = -\partial C/\partial_z$ ($C : S, T$), which can be inserted in Eq (10). Considering $D_T >> D_S$ one obtains

$$\Lambda(z,t) \sim \left(\frac{zS_0^2}{t^{3/2}T_0}\right)^{\frac{1}{2}}\exp\left[-z^2/(4D_S t)\right]. \quad (13)$$

Inserting β_C in inequality (7) and considering $D_T >> D_S$, one sees that this inequality holds for $z < h(t)$, where

$$h(t) = f(S_0, T_0)t^{1/2} \quad (14)$$

$$f(S_0, T_0) = 2D_S^{1/2}\,(\mathrm{In}(S_0/T_0) + \mathrm{In}\,q)^{1/2} \quad (15)$$

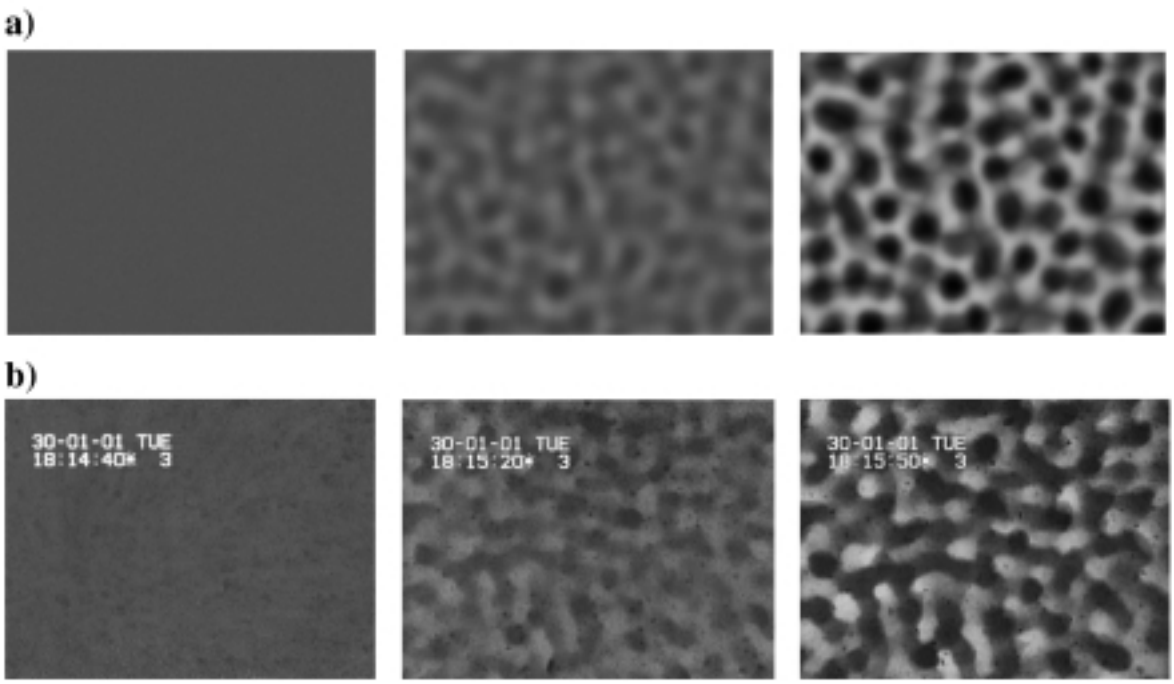

Fig 1. Self-organization of two homogeneous, horizontal layers. (a) Simulations using Eqs (1) through (5); from left to right: the first picture shows the homogeneous distribution at $t \approx 0$, the second one the first visible cells (t=80 s), and the third one (t=160 s) the fully formed cells with accumulation of S (darker spots) at the vertices. (b) Experiments using a layer of water above a layer of a solution of tenside (S) and glycerine (T) in water; the basis of the layers had dimensions 1.6 x1.2 mm; both layer heights were ≈ 0.3 mm; left picture: start with S=T=5 vol%; from left to right: t=30; 70; 100 s; light absorbtion causes S to appear dark.

$q = (\alpha_S/\alpha_T)(D_T/D_S)^{5/2}$. Considering Eqs (13), (14) and (15) one obtains

$$\int_0^{h(t)} \Lambda(z,t)dt \sim S_0 T_0^{-\frac{1}{2}} \left[\Gamma\left(\frac{3}{4}, 0\right) - \Gamma\left(\frac{3}{4}, \frac{(f(S_0, T_0)^2)}{4D_S}\right)\right], \quad (16)$$

with $\Gamma(x,a) = \int_a^\infty u^{x-1} e^{-u}\, du$. Note that the right hand side of Eq (16) is independent of time. For the ranges of S_0 and T_0 and for the parameters in our system, the Gamma function at the right in Eq (16) can be neglected, as compared to $\Gamma(\frac{3}{4}, 0)$. Thus,

$$\int_0^{h(t)} \Lambda(z,t)dz \sim S_0 T_0^{-\frac{1}{2}} \quad (17)$$

Inserting Eq (17) in Eq (9) yields

$$F \sim \exp\left[\int_0^{T_{em}} S_0 T_0^{-1/2} dt\right], \quad (18)$$

ie the scaling law

$$T_{em} \sim (\mathrm{In}\ F) S_0^{-1} T_0^{1/2}. \quad (19)$$

In order to estimate λ, we approximate $\beta_T(z, t)$ by its mean in the z-interval $[0, h(t)]$; inserting the result in Eq (11) and eliminating terms by considering the system parameters yields

$$\lambda \sim \left(\frac{t}{T_0}\right)^{\frac{1}{4}}. \quad (20)$$

Setting $t = T_{em}$ as given by the relation (19) finally renders the scaling law

$$\lambda \sim (\mathrm{In}\ F)^{\frac{1}{4}} T_0^{-\frac{1}{8}} S_0^{-\frac{1}{4}}. \quad (21)$$

Results and discussion.

Note that both scaling laws Eqs (19) and (21) have a well defined proportionality constant and a factor that depends on F. F, being defined as the factor by which fluctuations increase, depends on the initial fluctuations, which are unknown and may change from system to system, both in experiments and simulations. We therefore consider F as a parameter that is free to be adjusted in fitting procedures. The valuable information of Eqs (19) and (21) resides in the exponents of S_0 and T_0. In Fig 2 we test these scaling exponents (given by the slopes) and freely adjust F (given by the ordinate intercepts). The isolated diamonds in Fig 2 result from the integration of the PDE-system (Eqs (1)-(5)). The dotted straight lines display the scaling laws given by Eqs (19) and (21).

Fig 2a tests Eq (19) for $S_0 = T_0$; it thus tests $T_{em} \sim C_0^{-1/2}$ ($C_0 = T_0 = S_0$). Fig 2b tests Eq (19) at $S_0 = const.$; it thus tests $T_{em} \sim T_0^{1/2}$. Fig 2c tests Eq (19) at $T_0 = const$, thus testing $T_{em} \sim S_0^{-1}$. Fig 2d tests Eq (21) for $S_0 = T_0$, ie $\lambda \sim C_0^{-3/8}$, ($C_0 = T_0 = S_0$). Fig 2e tests Eq (21) for $S_0 = \mathrm{Const}$, ie $\lambda \sim T_0^{-1/8}$. Fig 2f tests Eq (21) for $T_0 = \mathrm{Const}$, ie $\lambda \sim S_0^{-1/4}$. Fig 3 tests Eq (20), ie $\lambda \sim t^{\frac{1}{4}}$. Note that the scaling laws only fail at the right of Fig 2f and fail slightly at the left of Fig 2e, which indicates that the approximations made in the previous section do not hold in those ranges.

Conclusions

The exponential dependences on S_0, T_0 and t, as given in Eqs (19), (20) and (21), satisfactorily describe the very complicated hydrodynamic processes contained in the partial differential equations (1)-(5). It is left to future work to verify these scaling exponents experimentally. In addition, the lines of thought presented here may serve, in the future, as a guide for other double-diffusive convective systems. In some of the systems mentioned in the Introduction (alloys, sewage, icebergs, stars or magma), the time of appearance T_{em} and the wavelength λ are observable quantities that characterize the processes in a global way. The existence of scaling laws, such as those presented here, are useful descriptions, insofar as they allow — for practical purposes — a considerable reduction of the systems' complexity.

Acknowledgements

We thank the Deutsche Forschungsgemeinschaft for financial support (Grants Ma 629/5-). Also, we thank Prof Dr R Winter for help with the X-ray small-angle scattering experiments.

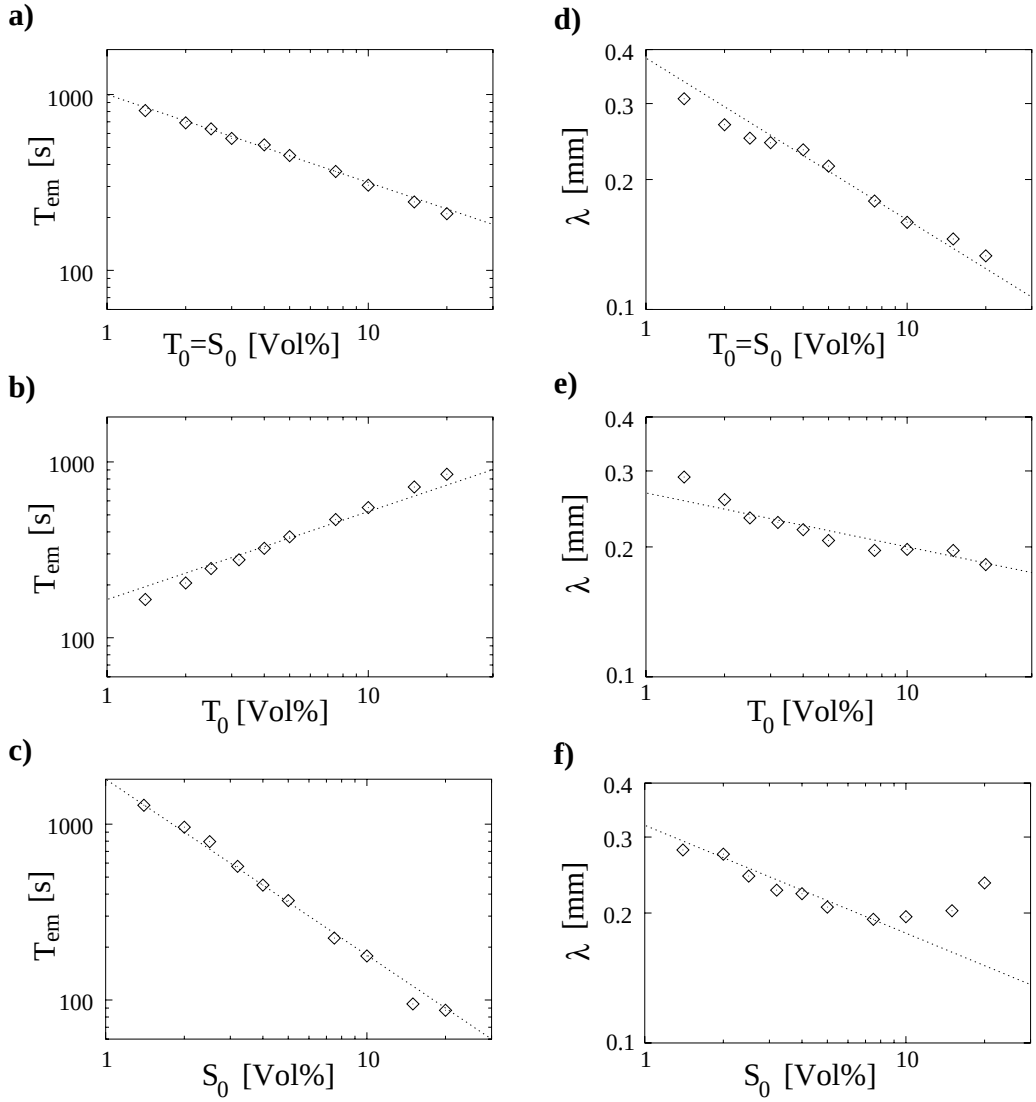

Fig 2. Solutions of partial differential equations (diamonds), as compared to exponential scaling laws (straight, dotted lines given by Eqs (19) and (20)). Ordinates: cell appearance time T_{em} in (a-c), wavelength λ at t=T_{em} in (d-f). Abscissas show the initial concentrations T_0, S_0: T_0=S_0 in (a,d),T_0 for S_0=5 vol% in (b,e), S_0 for T_0=5 vol% in (c,f).

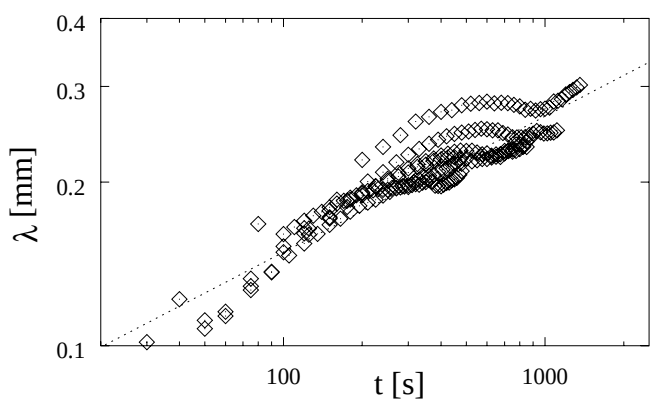

Fig 3. Time dependence of λ The diamonds are examples of results from PDE integration for T_0=5 Vol%, S_0=2, 2.5, 3.2, 3, 5, 7.5 Vol%. Dotted line: approximation given by Eq (20).

REFERENCES

1. Chen CF and Johnson DH (1984) Double-diffusion convection: a report on an engineering conference. *J Fluid Mech* 138, 405-16.
2. Huppert HE and Turner JS (1981) Double-diffusive convection. *J Fluid Mech* 106, 299-329.
3. Turner JS (1985) Multicomponent convection. *Ann Rev Fluid Mech* 17, 11-44.
4. Shirtcliffe TGL and Turner JS (1970) Observations of the cell structure of salt fingers. *J Fluid Mech* 41, 707-19.
5. Fisher H (1971) The dilution of an undersea sewage cloud by salt fingers. *Water Res* 5, 909-15.
6. Donaldson PB (1978) Melting of antarctic icebergs. *Nature* 275, 305-6.
7. Huppert HE and Turner JS (1978) Melting icebergs. *Nature* 271, 46-8.
8. Neshyba S (1978) On melting icebergs. *Nature* 275, 567.
9. Tait S and Jaupart C (1989) Compositional convection in viscous melts. *Nature* 338, 571-4.
10. Tait RI and Howe MR (1971) Thermohaline staircase. *Nature* 231, 178-9.
11. Williams AJ (1974) Salt fingers observed in the mediterranean outflow. *Science* 185, 941-3.
12. Schmitt J and Rossner R (1983) Double diffusive magnetic buoyancy instability in the solar interior. *Astrophys J* 265, 901-24.
13. Turner JS (1980) A fluid-dynamical model of differentiation and layering in magma chambers. *Nature* 285, 213-5.
14. Schmitt RW (1983), The characteristics of salt fingers in a variety of fluid systems, including stellar interiors, liquid metals, oceans and magmas. *Phys Fluids* 26, 2373-7.
15. Ferziger JH and Peric M (1997) Computational methods for fluid dynamics Springer.
16. Taylor J and Veronis G (1986) Experiments on salt fingers in a Hele-Shaw cell. *Science* 231, 39-41.
17. *Handbook of Surfactants* (Edited by Porter MR). Blackie Acad 1994.
18. *Methoden der biophysikalischen Chemie* (Edited by Winter R and Noll F), Teubner, 1998.
19. Linden PF (1973), On the structure of salt fingers. *Deep-Sea Research* 20, 325-40.
20. Taylor JR and Veronis G (1996), Experiments on double-diffusive sugar-salt fingers at high stability ratio. *J Fluid Mech* 321, 315-33.
21. Stern ME (1960), The "salt-fountain" and thermohaline convection. *Tellus* 12, 172-5.